Original Article

A simplified model for determining the cutting plane during thoracoscopic anatomical partial lobectomy of the right lower lobe

Yun Liu[1,2#], Bin Qiu[3#], Songlin Zhang[1,2], Chaobing Liu[1,2], Ming Yan[1,2], Lailong Sun[1,2], Dominique Gossot[4], Takahiro Homma[5], Fariha Sheikh[6], Peter J. Kneuertz[7]

[1]Department of Cardiothoracic Surgery, The First College of Clinical Medical Science, China Three Gorges University, Yichang, China; [2]Department of Cardiothoracic Surgery, Yichang Central People's Hospital, Yichang, China; [3]Department of Thoracic Surgery, National Cancer Center/National Clinical Research Center for Cancer/Cancer Hospital, Chinese Academy of Medical Sciences and Peking Union Medical College, Beijing, China; [4]Thoracic Department, Curie-Montsouris Thorax Institute-Institut Mutualiste Montsouris, Paris, France; [5]Department of General Thoracic and Cardiovascular Surgery, Graduate School of Medicine and Pharmaceutical Sciences, University of Toyama, Toyama, Japan; [6]Department of Surgery, Division of Trauma and Critical Care, Rutgers, New Jersey Medical School, Newark, New Jersey, USA; [7]Division of Thoracic Surgery, The Ohio State University Wexner Medical Center, Columbus, OH, USA

Contributions: (I) Conception and design: Y Liu, B Qiu; (II) Administrative support: S Zhang; (III) Provision of study materials or patients: Y Liu, B Qiu, S Zhang; (IV) Collection and assembly of data: Y Liu; (V) Data analysis and interpretation: Y Liu, B Qiu; (VI) Manuscript writing: All authors; (VII) Final approval of manuscript: All authors.

[#]These authors contributed equally to this work.

Correspondence to: Songlin Zhang, MD. Department of Cardiothoracic Surgery, The First College of Clinical Medical Science, China Three Gorges University, Yichang, China; Department of Cardiothoracic Surgery, Yichang Central People's Hospital, No. 183 Yiling Road, Yichang, China. Email: 278087836@qq.com.

Background: Few studies have examined the use of two-dimensional computed tomography (2D CT) and three-dimensional (3D) reconstruction images to determine the intersegmental plane (ISP) for pulmonary segmentectomy, but a systematic approach and nomenclature are currently lacking. This current study used 3D reconstruction of CT imaging to analyze variations in the right lower lobe's pulmonary ISP and created a simplified model to determine the optimum cutting plane (CP) for clinical application for operative planning and use during thoracoscopic anatomical partial lobectomy (APL).

Methods: Between January 2018 and October 2019, 325 patients with pulmonary lesions were identified who underwent thin-slice CT scans of the chest. The ISPs were identified by analyzing the 2D CT scans and 3D reconstruction images and the anatomical characteristics segmental boundary. The CP for the thoracoscopic procedure was then determined within the safe surgical margins, and a simplified CP model was created.

Results: The boundary between adjacent lung segment A and segment B was be expressed as "ISP: Sa-Sb". The ISP was divided into venous ISP (VISP), arterial ISP (AISP), and bronchial ISP (BISP). The proposed model of the CP can be expressed as follows: CP (f) = (V/A/B) ISP (x) + (V/A/B) sub ISP (y) + (V/A/B) sub-sub ISP (z).

Conclusions: This report is a first attempt to provide a nomenclature for identifying the ISP, and create a simplified model for determining the CP for thoracoscopic partial lobectomy.

Keywords: Segmentectomy; computed tomography (CT); three-dimensional reconstruction (3D reconstruction); intersegmental plane (ISP); cutting plane (CP)

Submitted Apr 15, 2021. Accepted for publication Jul 16, 2021.
doi: 10.21037/tlcr-21-525
View this article at: https://dx.doi.org/10.21037/tlcr-21-525

Introduction

Segmentectomy is a parenchyma sparing approach for anatomical pulmonary resection, applicable to a selected group of patients with early-stage lung cancer, and is typically performed by video-assisted thoracic surgery (VATS) (1). Anatomical partial lobectomy (APL) is a concept in oncology therapeutics based on the anatomy of the pulmonary segments and subsegments (2), APL may encompasses the resection of a single segment or multiple segments (extended segmentectomy), or a subsegmentectomy, but does not include non-anatomical procedures such as wedge resections. The procedure of APL entirely takes into account the individualized surgical differences of sub lobectomy in different patients based on tumor location. For multiple pulmonary nodules, APL may be a better option, especially for those located in different lobes (2). Each pulmonary segment is an independent unit, confined by anatomical boundaries called the intersegmental plane (ISP). The ISP is considered an ideal *cutting plane* (CP) to separate diseased from healthy lung segments in order to maximize resection margins length and to avoid leaving devitalized parenchyma. Inadequate determination and division of the ISP may lead to unsatisfactory oncological outcomes (3). Local recurrence after surgical resection is related to the range of the safety margin, and for which guidelines have been established (4-6).

In the physiological state, adjacent lung segments are separated by ISPs and are completely different in morphology and function. The ISP helps to locate lung lesions accurately and determine the extent of the lesions; it may even be valuable for identifying certain imaging manifestations of lung diseases. In 1956, Hamilton *et al*. noted that the connection between adjacent lung segments formed a "natural split line", and the segments could be completely separated along the line, indicating no lung tissue located on the actual line (7). The intersegmental septum consists of 3 layers: the deep layer is composed of loose connective tissue, and the alveolar walls of the two adjacent segments serve as the superficial layers (8). The ISP contains intersegmental veins, nerves, and lymphatic vessels. The intersegmental vein is an indirect marker of the intersegmental boundary as it runs along the ISP. The pulmonary segmental artery is located in the segment and does not cross the segment boundary, and thus, in theory, the segment boundary is a region with no pulmonary artery. As the segmental artery and the segmental bronchus are concomitant, there is no bronchus at the segmental plane level (*Figure 1*). In 3D reconstruction images, the intersegmental vein and its branches can be accurately identified, allowing the ISP to be easily recognized. Hence, based on the anatomical features of the ISP, 3D reconstruction images and 2D computed tomography (CT) images can be used to identify the ISP.

While there has been much research on developing methods to determine the optimal targeted lung segments during operations, imaging techniques to determine the lung CP have not been investigated in the clinical setting. Surgeons routinely depend on cross sectional imaging during operative planning to identify the target segment(s) and the anticipated resection margin. However, a systematic approach for capturing the ISP based on CT imaging is currently lacking. In this study, we used 3D reconstruction of CT images to analyze the anatomic boundaries of ISPs. We sought to establish an anatomic based nomenclature for ISPs and create simplified cutting plane model for use during VATS segmentectomy. We present the following article in accordance with the STROBE reporting checklist (available at https://dx.doi.org/10.21037/tlcr-21-525).

Methods

Patient characteristics and three-dimensional reconstruction

Between January 2018 and October 2019, 325 patients presented to the hospital with pulmonary lesions and underwent thin-slice (0.625–2 mm) CT scans of the lungs. 3D reconstruction images were generated for all patients using the Materialise 3-Matic software (developed by Materialise Nv Co., Materialise's interactive medical image control system, Kingdom of Belgium. Serial number: A51D56D6-C3XE-0011-1F7605D216DF39D5). The eligibility criteria for patients were as follows: (I) patients were clinically diagnosed with non-small cell lung cancer (NSCLC) by chest CT, and the total size of the lesion was 2 cm or less; (II) patients meeting indication for APL based on the National Comprehensive Cancer Network (NCCN) guidelines for NSCLC; (III) head magnetic resonance imaging (MRI), abdominal ultrasound (or CT), and bone scan or positron emission tomography (PET) were performed to exclude distant metastasis, and routine assessment of cardiopulmonary function was performed to exclude surgical contraindications; and (IV) no neoadjuvant chemotherapy or radiotherapy treatment had been administered. The study was conducted following

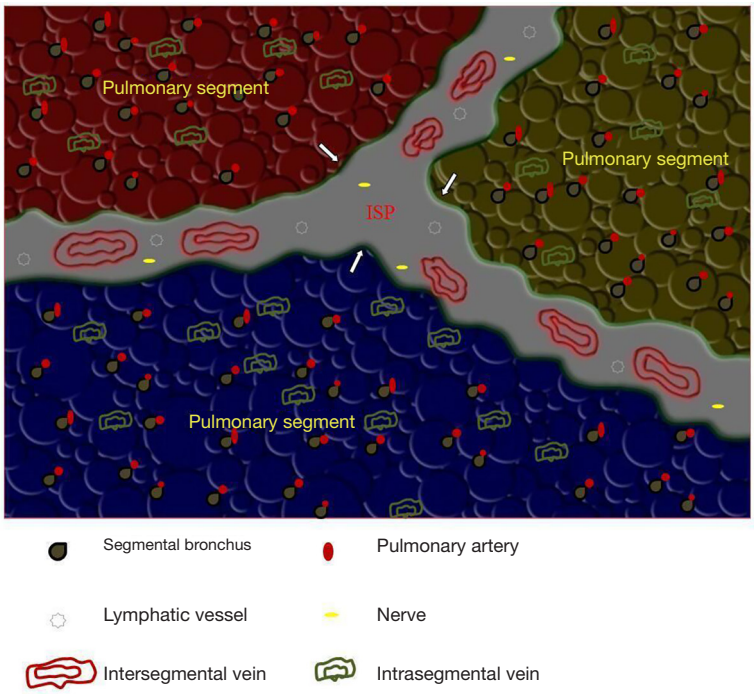

Figure 1 Simplified models of ISP. The deep layer is composed of loose connective tissue (gray areas). The alveolar walls of the 2 adjacent segments serve as the superficial layers (white arrow head). ISP, intersegmental plane.

Table 1 Number and verbal description of right lower lobe segments

Segment No.	Segment description
S6	Superior segment
S7	Medial basal segment
S8	Anterior basal segment
S9	Lateral basal segment
S10	Posterior basal segment
S*	Subsuperior segment
pS*	Posterior subsuperior segment
lS*	Lateral subsuperior segment
aS*	Anterior subsuperior segment

the Declaration of Helsinki (as revised in 2013). Informed consent was obtained from all patients. The protocol of this study was approved by the institutional review board of Yichang Central People's Hospital (No. HEC-KYJJ-2018-601-01).

The ISP of the right lower lobe

Based on the anatomic features of the ISP, 3D reconstruction images and the 2D CT scans can be combined to recognize the ISP of the right lower lobe with the intersegmental veins (V6b, V6c, V8b, and V9b) running along the ISP. ISPs always run between two tracheae of segments, and likewise, subsegment ISPs run between two tracheae of subsegments. This study proposes a standardized nomenclature to describe the plane between segment A and segment B with the abbreviation "ISP: Sa-Sb". To illustrate, the ISP between the right lower lobe S9 segment and S10 segment can be abbreviated as ISP: RS9-S10. There are six segments in the right lower lobe, and the segment numbers and the corresponding descriptions of the pulmonary ISPs are listed in *Table 1*. From the study cohort, a total of 14 ISPs were identified, and the names of the ISPs and their intersegmental veins are listed in *Table 2*. The variations in the right lower lobe ISPs were mainly related to the type of medial basal segmental bronchus (B7) and subsuperior segmental bronchus (B*).

Table 2 Right lower lobe segments intersegmental planes and intersegmental veins

Intersegmental planes	Intersegmental veins
ISP: RS6-S7	V6c
ISP: RS6-S8	V6b
ISP: RS6-S9	V6b
ISP: RS6-S10	V6c
ISP: RS7-S8	V7b
ISP: RS7-S9	Unnamed intersegmental vein
ISP: RS7-S10	Unnamed intersegmental vein
ISP: RS8-S9	V8b
ISP: RS9-S10	V9b
ISP: RS*-S6	Unnamed intersegmental vein
ISP: RS*-S7	Unnamed intersegmental vein
ISP: RS*-S8	Unnamed intersegmental vein
ISP: RS*-S9	Unnamed intersegmental vein
ISP: RS*-S10	Unnamed intersegmental vein

ISP, intersegmental plane.

The medial basal segmental bronchus (B7) and the ISP

The first bronchial segment that branches solely to the mediastinal side after the B6 branching is defined as B7. B7 divides into an anterior ramus B7a and a posterior ramus B7b. The B7a runs anterior to the inferior pulmonary vein (IPV), whereas B7b runs posterior to the IPV. Bronchial segments that showed medial branching from a portion of the double or triple branching of the basal bronchus were not regarded as B7, and these cases were processed as "no B7" cases. B7 is classified into 4 types according to the combination of B7a and B7b; that is, B7ab, B7a, B7b, and no B7 (*Figure 2*), with the B7a type being the most common (9,10).

The B7a type only comprises B7a, and in this type, S7 is located anterior to the IPV, and A7 branches from either the basal segmental artery or A8 and runs on the ventral side of the basal segmental bronchus to flow into S7. The B7b type only comprises B7b, and in this type, S7 is located posterior to the IPV, and the A7 branches flow in from either the basal segmental artery or A10. The B7ab type comprises B7a and B7b, and in this type, S7 is located both anterior and posterior to the IPV. The no B7 type represents the bronchial segment with pulmonary parenchyma in an area between B6 and the basal segment without extending into the medial basal segment (9). Different types of B7 led to different ISPs. For example, compared with the B7a type, in the B7b type, ISP: S7-S8 is not available, but ISP: S7-S10 can be observed.

The subsuperior bronchus (B) and the ISP*

The independent bronchus observed between B6 and B10 is called the subsuperior bronchus (B*) (9,10), and it runs posteriorly or posterolaterally but not anteriorly or laterally (11,12). However, the atypical bronchi originating from the stem bronchi frequently spread anteriorly or laterally, and herein, it is designated as an atypical B*. The B* can be classified into 3 types according to the direction: posterior B* (pB*, between B6 and B10; known as the narrow sense of B*), lateral B* (lB*, between B6 and B9), and anterior B* (aB*, between B6 and B8; *Figure 3*). The independent segment that is observed between S6 and S8, S6 and S9, or S6 and S10 is called the subsuperior segment (S*), and it has an independent segmental bronchus (B*), artery (A*), and vein (V*). The pattern of the V* is complex and frequently drains into V6 or V10.

When the B* is present, the ISP changes. For example, with the posterior B* (pB, between B6 and B10), the ISP: S6-S10 is not available, but ISP: pS*-S6, ISP: pS*-S10, ISP: pS*-S9, and ISP: pS*-S7 can be detected. V6c is no longer an intersegmental vein between S6 and S10 but an intersegmental vein of S6 and pS*. For the lB*, S6-lS*, S7-lS*, S8-lS*, S9-lS*, and S10-lS* can be detected, while ISP: S6-S9 is absent. For the aB*, ISP: S6-aS*, S7-aS*, S8-aS*, and Sa*-S9 can be detected, while ISP: S6-S8 is absent.

The cutting plane and the ISP

The ISP is an objective anatomical structure and can be divided into the venous ISP (VISP), arterial ISP (AISP), and bronchial ISP (BISP) (13). During operation, the VISP, AISP, and BISP can show different boundaries. However, the ISP is defined as a 3D area comprising the minimum area, including the arterial, venous, and bronchial drainage boundaries. The venous plane is the largest, and the bronchial plane is the smallest. As the intraoperative boundary may be the artery watershed boundary, the vein watershed boundary, or the tracheal watershed boundary, it may not be accurate to refer to it generally as the ISP. Therefore, in this study, the boundary between the target segment and the reserved segment produced during the operation was referred to as the cutting plane (CP), and the target segment was cut along the CP. The CP has unique anatomical characteristics and clinical significance that

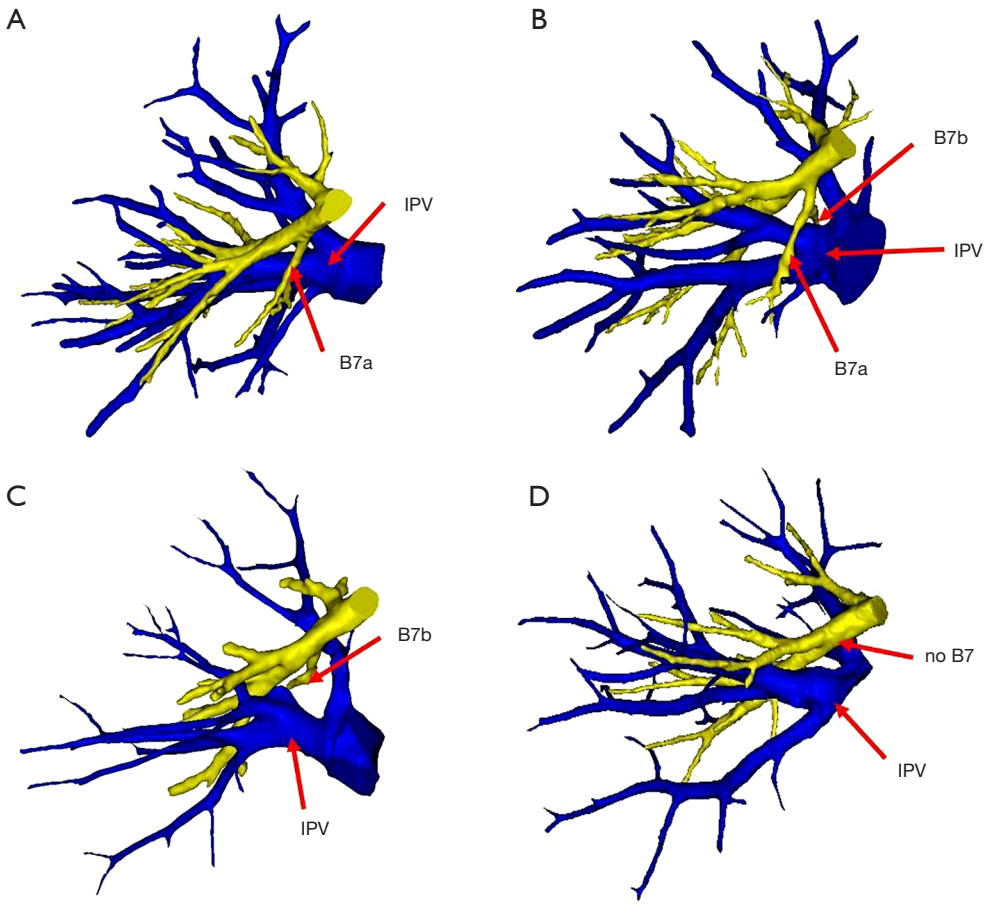

Figure 2 Branching patterns of B7 in the right lower lobe. (A) B7a type; (B) B7ab type; (C) B7b type; (D) no B7 type. IPV, inferior pulmonary vein.

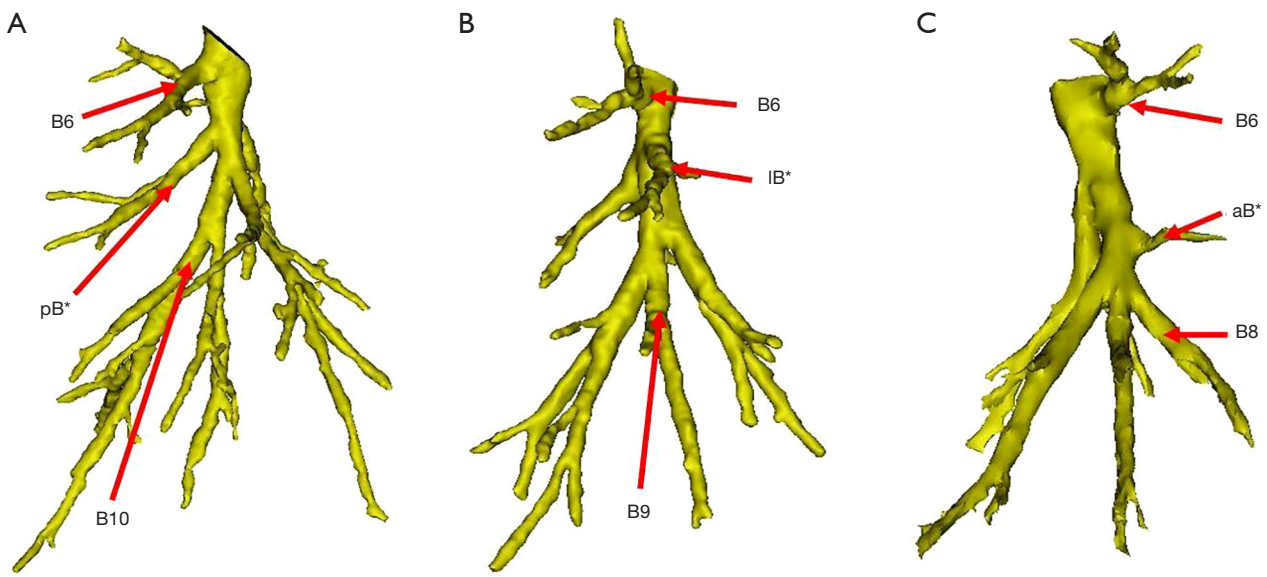

Figure 3 The B* can be classified into 3 types according to directions. (A) Posterior B* (pB*, between B6 and B10); (B) lateral B* (lB*, between B6 and B9); (C) anterior B* (aB*, between B6 and B8).

Table 3 Baseline characteristics of patients

Characteristic	Value
Age (years), median [range]	66.3 [26–82]
Male/female, n	146/179
Active smokers, n	147
BMI (kg/m^2), median [range]	22.9 [20.5–25.6]
Image characteristics	
Size (mm), median [range]	15.7 [8–20]
Pure GGN, n	77
GGN with <50% solid part, n	248

BMI, body mass index; GGN, ground glass nodule.

differs from those of the ISP.

Statistical analysis

All data were expressed as mean ± standard deviations (SD). Statistical analysis was performed using Statistical Package for the Social Sciences software version 23.0 for Windows (SPSS Inc., Chicago, IL, USA). Student's *t*-test or Wilcoxon test was used to compare quantitative continuous data. Chi-square or Fisher's exact test was used when required for dichotomous or categorical variables. A P value of less than 0.05 was considered statistically significant.

Results

The characteristics of the patients are summarized in *Table 3*. The 325 patients included 146 men (44.9%) and 179 women (55.1%), aging from 26 to 82 years (median 66.3 years). Of the lesions, 77 (23.7%) were pure ground glass nodules (pGGNs) and 248 (76.3%) were part-solid nodules (PSNs). All pulmonary nodules were detected by regular physical examination or CT screening. Complete 3D segmental models were successfully reconstructed in all 325 patients. The IPSs of every patient were identified by 2D CT scan combined with 3D reconstruction. The most common type of ISP was the B7a type, which was detected in 55.1% of cases (179 cases).

B7 and ISPs

The ISPs for B7a included: S6-S7, S6-S8, S6-S9, S6-S10, S7-S8, S7-S9, S8-S9, and S9-S10. The B7ab type was observed in 98 cases (30.2%). The ISPs for B7ab included: S6-S7, S6-S8, S6-S9, S6-S10, S7-S8, S7-S9, S7-S10, S8-S9, and S9-S10. The B7b type was observed in 41 cases (12.6%). The ISPs for B7b included: S6-S7, S6-S8, S6-S9, S6-S10, S7-S9, S7-S10, S8-S9, and S9-S10. The no B7 type was observed in 7 cases (2.2%), and the ISPs included: S6-S8, S6-S9, S6-S10, S8-S9, and S9-S10 (*Table 4*).

B and ISPs*

The independent segmental bronchus of the broad sense S* is B*, and this can be classified into three subtypes (pB*, lB*, and aB*). The pB* subtype was detected in 34 cases (10.4%). ISP: S6-pS*, S7-pS*, S9-pS*, and S10-pS* were detected in 34 cases (10.4%). However, ISP: S6-S10 was absent. The lB* subtype was detected in 15 cases (4.6%); and ISP: S6-lS*, S7-lS*, S8-lS*, S9-lS*, and S10-lS* were detected in 15 cases (4.6%), with ISP: S6-S9 not being observed. The aB* subtype was detected in 6 cases (1.8%); and ISP: S6-aS*, S7-aS*, S8-aS*, and S9-aS* were detected in 6 cases (1.8%), with ISP: S6-S8 going undetected (*Table 4*).

B and B7*

pB*-B7a was detected in 18 cases (5.5%), pB*-B7ab was detected in 9 cases (2.8%), pB*-B7b was detected in 6 cases (1.8%), and pB*-no B7 was detected in 1 case (0.3%). lB*-B7a was detected in 7 cases (2.2%), lB*-B7ab was detected in 5 cases (1.5%), lB*-B7b was detected in 2 cases (0.6%), and lB*-no B7 was not detected. aB*-B7a was detected in 3 cases (0.9%), aB*-B7ab was detected in 1 case (0.3%), aB*-B7b was detected in 2 cases (0.6%), and aB*-no B7 was not detected. The frequency of pB *-B7a was significantly higher than that of the other combinations (*Table 5*).

The model of the CP

The ISP can be divided into the ISPs of venous drainage, artery drainage, and bronchus drainage. The CP is composed of different ISPs. The model of the CP can be expressed as follows: CP (f) = (V/A/B) ISP (x) + (V/A/B) sub ISP (y) + (V/A/B) sub-sub ISP (z). For example, the CP of APL (RS8 + RS6ii resection) is as follows: CP (RS8 + RS6ii) = ISP: RS9-RS8 + Sub ISP: RS7a-RS8 + sub-sub ISP: RS6bi-RS6bii + sub-sub ISP: RS6bii-RS7a (*Figure 4*).

Discussion

Compared with traditional lobectomy, APL can preserve a

Table 4 The ISPs of the right lower lobe and the type of B7and B*

Type	n (%)	The ISPs of right lower lobe
B7		
B7a	179 (55.1)	ISP: S6-S7, S6-S8, S6-S9, S6-S10, S7-S8, S7-S9, S8-S9, S9-S10
B7ab	98 (30.2)	ISP: S6-S7, S6-S8, S6-S9, S6-S10, S7-S8, S7-S9, S7-S10, S8-S9, S9-S10
B7b	41 (12.6)	ISP: S6-S7, S6-S8, S6-S9, S6-S10, S7-S9, S7-S10, S8-S9, S9-S10
No B7	7 (2.2)	ISP: S6-S8, S6-S9, S6-S10, S8-S9, S9-S10
B*		
No B*	270 (83.1)	ISP: S6-S7, S6-S8, S6-S9, S6-S10, S7-S8, S7-S9, S7-S10, S8-S9, S9-S10
pB*	34 (10.5)	New additions ISP: S6-pS*, S7-pS*, S9-pS*, S10-pS*
		Disappearing ISP: S6-S10
lB*	15 (4.6)	New additions ISP: S6-lS*, S7-lS*, S8-lS*, S9-lS*, S10-lS*
		Disappearing ISP: S6-S9
aB*	6 (1.8)	New additions ISP: S6-aS*, S7-aS*, S8-aS*, S8-S9, aS*-S9
		Disappearing ISP: S6-S8

Table 5 The ISPs of the right lower lobe and the B7-B* type

Type	n (%)	The ISPs of right lower lobe
pB*-B7a	18 (5.5)	ISP: S6-S7, S6-S8, S6-S9, S6-pS*, S7-S8, S7-S9, S8-S9, S9-pS*, S9-S10, S10-pS*
pB*-B7ab	9 (2.8)	ISP: S6-S7, S6-S8, S6-S9, S6-pS*, S7-S8, S7-S9, S7-pS*, S7-S10, S8-S9, S9-pS*, S9-S10, S10-pS*
pB*-B7b	6 (1.8)	SP: S6-S7, S6-S8, S6-S9, S6-pS*, S7-S9, S7-pS*, S7-S10, S8-S9, S9-pS*, S9-S10, S10-pS*
pB*-no B7	1 (0.3)	ISP: S6-S8, S6-S9, S6-pS*, S8-S9, S9-pS*, S9-S10, S10-pS*
lB*-B7a	7 (2.2)	ISP: S6-S7, S6-S8, S6-lS*, S6-S10, S7-S8, S7-S9, S7-lS*, S8-S9, S8-lS*, S9-S10, S9-lS*, S10-lS*
lB*-B7ab	5 (1.5)	ISP: S6-S7, S6-S8, S6-lS*, S6-S10, S7-S8, S7-S9, S7-lS*, S7-S10, S8-S9, S8-lS*, S9-S10, S9-lS*, S10-lS*
lB*-B7b	2 (0.6)	ISP: S6-S7, S6-S8, S6-lS*, S6-S10, S7-S9, S7-lS*, S7-S10, S8-S9, S8-lS*, S9-S10, S9-lS*, S10-lS*
lB*-no B7	0	ISP: S6-S8, S6-lS*, S6-S10, S8-S9, S8-lS*, S9-S10, S9-lS*, S10-lS*
aB*-B7a	3 (0.9)	ISP: S6-S7, S6-aS*, S6-S9, S6-S10, S7-S8, S7-aS*, S7-S9, S8-aS*, S8-S9, aS*-S9, S9-S10
aB*-B7ab	1 (0.3)	ISP: S6-S7, S6-aS*, S6-S9, S6-S10, S7-S8, S7-aS*, S7-S9, S7-S10, S8-aS*, S8-S9, aS*-S9, S9-S10
aB*-B7b	2 (0.6)	ISP: S6-S7, S6-aS*, S6-S9, S6-S10, S7-S9, S7-S10, S8-aS*, S8-S9, aS*-S9, S9-S10
aB*-no B7	0	ISP: S6-aS*, S6-S9, S6-S10, S8-aS*, S8-S9, aS*-S9, S9-S10

greater degree of lung function and may be used for both benign diseases and malignant tumors. The difficulty of APL is more significant than that of lobectomy for the reason that the anatomy of lung segments, especially sub-segments, are more complicated. Vascular and bronchial variations of lung segments are common. The vessels are thinner and more fragile so that more difficult to denude. With malignant lung tumors, segmental resection is mainly suitable for patients who are not candidates for lobectomy or a selective group of patients with small peripheral tumors. Some studies have shown that segmental resection and lobectomy may achieve the same treatment effect for very early stage lung cancer (stage 1a) patients in well selected patients. The accurate determination of the plane between segments and the cutting edge distance are key factors that affect the long-term therapeutic benefits of

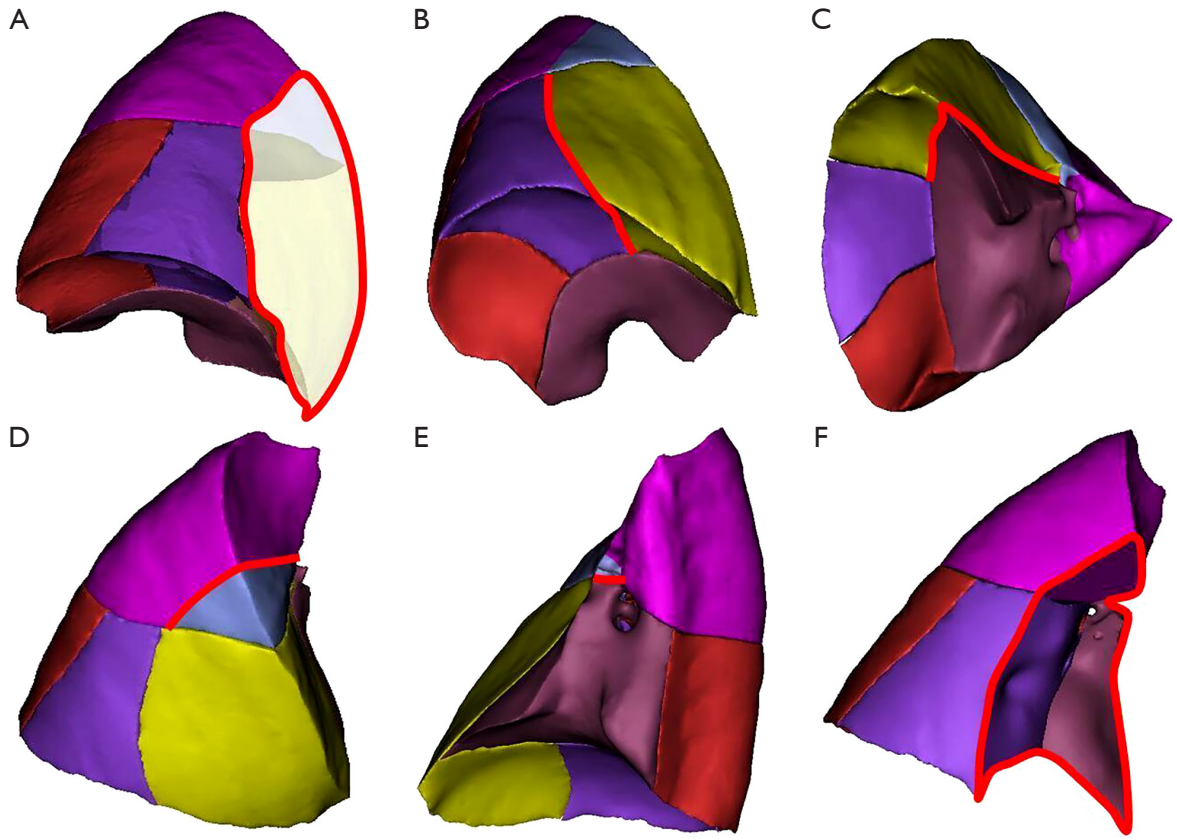

Figure 4 The cutting plane of RS8 + RS6bii segmentectomy. (A) APL: RS8 + RS6bii; (B) ISP: RS9-RS8; (C) Sub ISP:RS7a-RS8; (D) sub-sub ISP: RS6bi-RS6bii; (E) sub-sub ISP: RS6bii-RS7a; (F) CP (RS8 + RS6bii) = ISP: RS9-RS8 + Sub ISP:RS7a-RS8 + sub-sub ISP: RS6bi-RS6bii + sub-sub ISP: RS6bii-RS7a. ISP, intersegmental plane.

pulmonary segmental resection (14,15). A clear demarcation of the ISP can guide the tailoring of the ISP and is necessary to achieve a high surgical success rate.

The pulmonary septum is composed of the alveolar wall and the fibrous connective tissue between the adjacent pulmonary segments. It can accommodate the veins, nerves, and lymphatics between the segments and separate the adjacent pulmonary segments. However, there are no visible fissures similar to oblique fissures or horizontal fissures on the ISPs. 3D reconstruction can identify the anatomical structures of bronchi, arteries, and veins of pulmonary segments and the relationships between the lesion and the surrounding structures. It can more accurately determine the intersegmental vein and its branches, and indeed, these veins can serve as an indirect landmark of ISPs. As the intersegmental vein runs along with the ISP, the first step is to identify the intersegmental vein. The curved surface of all the intersegmental veins forms the boundary of the lung segment.

In most cases examined in our study, 9 ISPs could be identified in the right lower lobe. Accurately determining each ISP position on 2D CT and 3D reconstruction images could help determine the scope of the resection and assist in the preoperative phase when planning the operation. To avoid confusion, this report proposed a simple but universal nomenclature for referring to the plane between two segments, namely, “ISP: Sa-Sb”.

In the 3D reconstruction images, B7 and B* had a significant impact on the right lower lung ISP. Systematic 3D analyses of the B7 of the right lower lung were performed, and the discrepancies between this current study and those of previous reports were examined. The B7ab type was observed in 98 cases (30.2%) with the frequency significantly less than that reported by Nagashima *et al.* (74.8%; P=0.001) (10), but significantly more frequent than that reported by Ferry and Boyden (58%; P<0.001) (11). The B7b type was observed in 41 cases (12.6%), representing a frequency much higher

than that detected in previous reports (4.8% reported by Nagashima *et al.*; P<0.001) (10).

The types of B7 varied, and the types and number of ISPs related to S7 also differed. This is the first study to report the influence of B7 on ISPs. Furthermore, in the reconstruction process and traditional subsuperior segments, some atypical subsuperior lung segments were detected, and these varied in their location. In this report, the traditional subsuperior segments were referred to as subsuperior segments in the narrow sense. The atypical subsuperior segments together with the subsuperior segments in the narrow sense were referred to as subsuperior segments in the broad sense. The B* could be classified into 3 types according to the directions, pB*, lB*, and aB*. In our data, B* was detected in 55 cases (16.9%), including pB* in 34 cases (10.4%), lB* in 15 cases (4.6%), and aB* in 6 cases (1.8%). The pB* subtype was detected in 34 cases (10.4%) at a frequency significantly lower than that reported in previous studies (20.4% reported by Nagashima *et al.*, P<0.001; 48% reported by Ferry and Boyden, P<0.001) (10,11). This is the first time broad sense B* and narrow sense B* have been defined.

The current methods of identifying the ISP are based on either the bronchial or the vascular territory. The bronchial plane is demarcated by using ventilatory techniques by creating an inflation/deflation zone or by injecting a dye into the segmental bronchus (10). The vascular ISP identification techniques are based on the arterial or venous territory. Thus, the two planes are inconsistent. A recent study confirmed this phenomenon: specifically, the target lung segment's volume divided according to the segment bronchial drainage area is the smallest, followed by the target artery, and the target vein is the largest (13). This study suggested that the ISP is not an anatomically fixed plane, but rather, it is an area distributed according to the vascular drainage area. Therefore, a "cutting plane" determined according to the tumor's safe margin range and the corresponding vascular structure to be treated may be a more suitable method in the clinical setting (16,17). For example, during RS8 segmentectomy, the modified inflation-deflation method was used to identify the CP. After the targeted segment structures were dissected, the collapsed lung was initiated by full re-expansion with controlled airway pressure under 20 cmH_2O, followed by single-lung ventilation. After approximately 15 minutes, an irregularly curved demarcation was identified naturally between the deflated preserving segments and the inflated target segment. The V7b was not disconnected, and the plane between S7 and S8 was determined to be the arterial plane; V8b was not retained, and the plane between S8 and S9 was determined to be the venous plane; V6b was retained, and the plane between S6B and S8A was determined to be the arterial plane. Therefore, CP (f) = (A) ISP: S7-S8 + (V) ISP: S8-S9 + (A) sub-ISP: S6b-S8a. If the inflation-deflation method were used to identify the CP after the targeted segment structures were dissected, bilateral lung ventilation would commence. The irregularly curved demarcation would be used to naturally identify the deflated target segment and the inflated preserving segments. Thus, CP (f) = (B) ISP: S7-S8 + (B) ISP: S8-S9 + (B) sub ISP: S6b-S8a. The model of the CP can be expressed as follows: CP (f) = (V/A/B) ISP (x) + (V/A/B) sub ISP (y) + (V/A/B) sub-sub ISP (z).

Conclusions

Intersegmental pulmonary planes of the right lower lobe can be analyzed systematically using reconstruction of CT imaging and described with a simple and clear nomenclature. A subsuperior segments can be distinguished. The ISPs may be used to define cutting planes using a simplified model that may be used for operative planning prior to right lower lobe APL.

Acknowledgments

The authors appreciate the academic support from AME Thoracic Surgery Collaborative Group.

Funding: This study is supported by the Medical and Health Research Program (A20-2-015), Science & Technology Bureau of Yichang.

Footnote

Reporting Checklist: The authors have completed the STROBE reporting checklist. Available at https://dx.doi.org/10.21037/tlcr-21-525

Data Sharing Statement: Available at https://dx.doi.org/10.21037/tlcr-21-525

Conflict of Interest: All authors have completed the ICMJE uniform disclosure form (available at https://dx.doi.org/10.21037/tlcr-21-525). Dr. DG reported fees received from Delacroix-Chevalier (2000 Euros in 2020), Medtronic (500 euros in 2020), Ethcon (500 Euro in 2021s). The other

authors have no conflicts of interest to declare.

Ethical Statement: The authors are accountable for all aspects of the work in ensuring that questions related to the accuracy or integrity of any part of the work are appropriately investigated and resolved. The study was conducted in accordance with the Declaration of Helsinki (as revised in 2013). The protocol of this study was approved by the institutional review board of Yichang Central People's Hospital (No. HEC-KYJJ-2018-601-01). Informed consent was obtained from the patient before surgery.

References

1. Suzuki K, Saji H, Aokage K, et al. Comparison of pulmonary segmentectomy and lobectomy: Safety results of a randomized trial. J Thorac Cardiovasc Surg 2019;158:895-907.
2. Gao S, Qiu B, Li F, et al. Comparison of thoracoscopic anatomical partial-lobectomy and thoracoscopic lobectomy on the patients with pT1aN0M0 peripheral non-small cell lung cancer. Zhonghua Wai Ke Za Zhi 2015;53:727-30.
3. Mehta M, Patel YS, Yasufuku K, et al. Near-infrared mapping with indocyanine green is associated with an increase in oncological margin length in minimally invasive segmentectomy. J Thorac Cardiovasc Surg 2019;157:2029-35.
4. El-Sherif A, Fernando HC, Santos R, et al. Margin and local recurrence after sublobar resection of non-small cell lung cancer. Ann Surg Oncol 2007;14:2400-5.
5. Koike T, Koike T, Yoshiya K, et al. Risk factor analysis of locoregional recurrence after sublobar resection in patients with clinical stage IA non-small cell lung cancer. J Thorac Cardiovasc Surg 2013;146:372-8.
6. Koike T, Goto T, Sato S, et al. Radical segmentectomy as a potential alternative surgical treatment with curative intent in early-stage non-small cell lung cancer. J Thorac Dis 2020;12:6115-9.
7. Hamilton WJ. Textbook of human Anatomy. New York: ST Martin's, 1956.
8. Zuo YZ, Liu C, Liu SW. Pulmonary intersegmental planes: imaging appearance and possible reasons leading to their visualization. Radiology 2013;267:267-75.
9. Chujo M, Anami K. Branching patterns of segmental bronchi and arteries in the medial basal segment. J Bronchology Interv Pulmonol 2014;21:192-8.
10. Nagashima T, Shimizu K, Ohtaki Y, et al. Analysis of variation in bronchovascular pattern of the right middle and lower lobes of the lung using three-dimensional CT angiography and bronchography. Gen Thorac Cardiovasc Surg 2017;65:343-9.
11. Ferry RM Jr, Boyden EA. Variations in the bronchovascular patterns of the right lower lobe of fifty lungs. J Thorac Surg 1951;22:188-201.
12. Patnaik VV, Saha JC. Incidence of subsuperior bronchusmorphological and bronchographic study. Journal of the Anatomical Society of India 1999;48:99-104.
13. Sarsam M, Glorion M, de Wolf J, et al. The role of three-dimensional reconstructions in understanding the intersegmental plane: an anatomical study of segment 6. Eur J Cardiothorac Surg 2020;58:763-7.
14. Dai C, Shen J, Ren Y, et al. Choice of Surgical Procedure for Patients With Non-Small-Cell Lung Cancer ≤ 1 cm or > 1 to 2 cm Among Lobectomy, Segmentectomy, and Wedge Resection: A Population-Based Study. J Clin Oncol 2016;34:3175-82.
15. Zhao X, Qian L, Luo Q, et al. Segmentectomy as a safe and equally effective surgical option under complete video-assisted thoracic surgery for patients of stage I non-small cell lung cancer. J Cardiothorac Surg 2013;8:116.
16. Qiu B, Ji Y, He H, et al. Three-dimensional reconstruction/personalized three-dimensional printed model for thoracoscopic anatomical partial-lobectomy in stage I lung cancer: a retrospective study. Transl Lung Cancer Res 2020;9:1235-46.
17. Zhang M, Mao N, Wu QC, et al. Vein or artery-first resection in right middle lobe segmentectomy: which preserves more lung? Interact Cardiovasc Thorac Surg 2021;32:993-5.

Cite this article as: Liu Y, Qiu B, Zhang S, Liu C, Yan M, Sun L, Gossot D, Homma T, Sheikh F, Kneuertz PJ. A simplified model for determining the cutting plane during thoracoscopic anatomical partial lobectomy of the right lower lobe. Transl Lung Cancer Res 2021;10(7):3203-3212. doi: 10.21037/tlcr-21-525

